



**HAL**  
open science

## Magnetic flux expulsion from the core as a possible cause of the unusually large acceleration of the north magnetic pole during the 1990s

A. Chulliat, Hulot Gauthier, L. R. Newitt

► **To cite this version:**

A. Chulliat, Hulot Gauthier, L. R. Newitt. Magnetic flux expulsion from the core as a possible cause of the unusually large acceleration of the north magnetic pole during the 1990s. *Journal of Geophysical Research: Solid Earth*, 2010, 115 (B7), pp.B07101. 10.1029/2009JB007143 . insu-01288849

**HAL Id: insu-01288849**

**<https://insu.hal.science/insu-01288849>**

Submitted on 15 Mar 2016

**HAL** is a multi-disciplinary open access archive for the deposit and dissemination of scientific research documents, whether they are published or not. The documents may come from teaching and research institutions in France or abroad, or from public or private research centers.

L'archive ouverte pluridisciplinaire **HAL**, est destinée au dépôt et à la diffusion de documents scientifiques de niveau recherche, publiés ou non, émanant des établissements d'enseignement et de recherche français ou étrangers, des laboratoires publics ou privés.



# Magnetic flux expulsion from the core as a possible cause of the unusually large acceleration of the north magnetic pole during the 1990s

A. Chulliat,<sup>1</sup> G. Hulot,<sup>1</sup> and L. R. Newitt<sup>2</sup>

Received 17 November 2009; revised 2 March 2010; accepted 10 March 2010; published 10 July 2010.

[1] The north magnetic pole (NMP) has been drifting in a north-northwesterly direction since the 19th century. Both local surveys and geomagnetic models derived from observatory and satellite data show that the NMP suddenly accelerated during the 1990s. Its speed increased from about 15 km/yr in 1989 to about 60 km/yr in 2002, after which it started to decrease slightly. Using a Green's function, we show that this acceleration is mainly caused by a large, negative secular variation change in the radial magnetic field at the core surface, under the New Siberian Islands. This change occurs in a region of the core surface where there is a pair of secular variation patches of opposite polarities, which we suggest could be the signature of a so-called "polar magnetic upwelling" of the type observed in some recent numerical dynamo simulations. Indeed, a local analysis of the radial secular variation and magnetic field gradient suggests that the secular variation change under the New Siberian Islands is likely to be accompanied by a significant amount of magnetic diffusion, in agreement with such a mechanism. We thus hypothesize that the negative secular variation change under the New Siberian Islands that produced the NMP acceleration could result from a slowdown of the polar magnetic upwelling during the 1990s. We finally note that the NMP drift speed is determined by such a combination of factors that it is at present not possible to forecast its future evolution.

**Citation:** Chulliat, A., G. Hulot, and L. R. Newitt (2010), Magnetic flux expulsion from the core as a possible cause of the unusually large acceleration of the north magnetic pole during the 1990s, *J. Geophys. Res.*, 115, B07101, doi:10.1029/2009JB007143.

## 1. Introduction

[2] The north magnetic pole (NMP) is defined as the point on the Earth's surface where the geomagnetic field is directed vertically downward. Since its first direct observation by Ross in 1831 [Ross, 1834], the NMP has been located in the Canadian Arctic and has been drifting in a north-northwesterly direction. After more than a century and a half of slow drift at less than 15 km/yr, the NMP suddenly accelerated around 1990. This phenomenon was first detected through local surveys [Newitt and Barton, 1996; Newitt *et al.*, 2002] and later in global geomagnetic models [Mandea and Dormy, 2003]. According to the most recent direct observation of the NMP, made in April 2007, the NMP's drift rate has since stabilized at just over 50 km/yr [Newitt and Chulliat, 2007; Newitt *et al.*, 2009, hereafter NCO09]. It may even have started to decrease, as suggested by the recent xCHAOS geomagnetic field model which is based on data from the Ørsted and CHAMP satellites [Olsen and Mandea, 2007a].

[3] The NMP's drift is a particular manifestation of the geomagnetic secular variation, which originates in the Earth's outer core. It has been suggested that some aspects of the NMP's behavior could be related to geomagnetic jerks [Newitt *et al.*, 2002; Mandea and Dormy, 2003], jumps in the second derivative of magnetic components recorded at magnetic observatories [Courtillot *et al.*, 1978]. However, the April 2007 survey [NCO09] showed that the acceleration that occurred during the 1990s was much larger than all other recorded acceleration episodes since 1831, and although a geomagnetic jerk occurred around 1991 [Macmillan, 1996], its magnitude was comparable to that of previous and later jerks. Thus, a geomagnetic jerk cannot be the sole cause of the sudden and unusually large acceleration that the NMP underwent after 1990. As an alternative explanation, Olsen and Mandea [2007a] recently speculated that the NMP's sudden acceleration could be caused by its drifting above a large reversed flux patch at the core surface. However, they also warned that "linking the dip poles at the Earth's surface to the magnetic field at the core-mantle boundary must be taken with caution", and indeed did not provide any quantitative support for their claim.

[4] In the present paper, we revisit this problem in a more quantitative way. We examine NMP positions obtained from local surveys as well as positions obtained from recent geomagnetic field models, and we link the motion of the

<sup>1</sup>Equipe de Géomagnétisme, Institut de Physique du Globe de Paris, Université Paris Diderot, INSU, CNRS, Paris, France.

<sup>2</sup>Boreal Language and Science Services, Ottawa, Ontario, Canada.

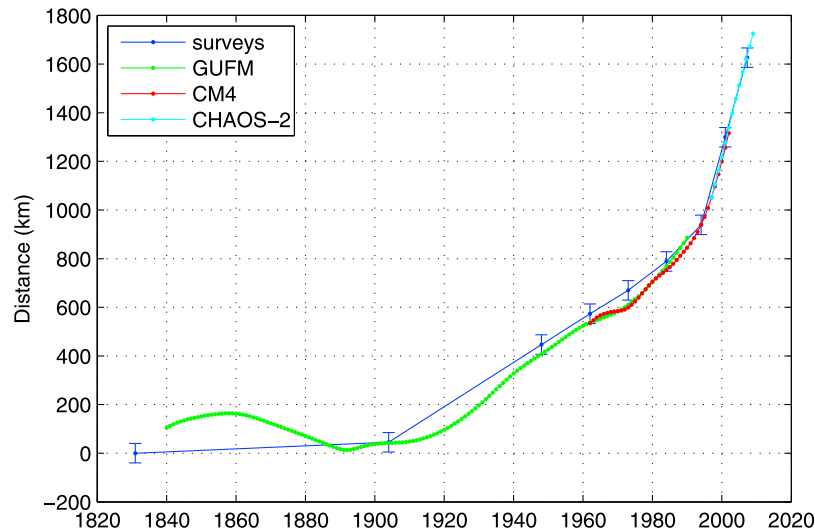


**Figure 1.** Geodetic distances (in km) from the 1831 position of the NMP to the observed positions (in blue) and the positions calculated from three time-varying main field models: *gufm1* (in green), CM4 (in red) and CHAOS-2 (in light blue). Estimated error bars for the observed NMP positions are shown.

NMP on the Earth's surface to the magnetic field at the core-mantle boundary by calculating an appropriate Green's function for the Neumann problem. Our goal is to identify precisely the core surface processes that constitute the origin of the large acceleration in the NMP's drift. We will show that this acceleration is mainly caused by an episode of unusually large change in the secular variation in a region of the core surface located under the New Siberian Islands, and that this change is possibly caused by magnetic flux expulsion from the core.

[5] The paper is organized as follows. In section 2, the NMP's drift speed since 1831 is reviewed. In section 3, the relationship between the acceleration of the NMP after 1990 and the secular variation in the polar region is analyzed. In section 4, the Green's function formalism is used to determine the changes in the magnetic field at the core surface which constitute the origin of the NMP's acceleration and these changes are interpreted in terms of core processes. The results are discussed in section 5.

## 2. Drift of the North Magnetic Pole Since 1831

[6] Figure 5 of NCO09 shows that the NMP has been drifting in an almost constant north-northwesterly direction since 1831. Therefore, the geodetic distance between the position of the NMP at any given time and the 1831 position is a good approximation of the distance covered by the NMP during that time interval. This is shown in Figure 1 for the eight NMP positions obtained by surveying the field in the NMP vicinity between 1904 and 2007 (see NCO09 for the list of observed positions since 1831). The plotted error bars correspond to a 40 km positional uncertainty, which was estimated by NCO09 for the 2007 NMP position.

[7] Figure 1 also shows the distances between the 1831 position and NMP positions calculated from three time-varying main field models: the *gufm1* model [Jackson *et al.*, 2000], the CM4 model [Sabaka *et al.*, 2004] and the CHAOS-2 model [Olsen *et al.*, 2009]. Although the *gufm1*

model covers the time period 1590 to 1990, we used it only to calculate NMP positions after 1840, since intensity observations were not available for inclusion in the data set prior to that year. The model is based on surface data collected aboard ships (19th century), survey data, observatory data, and data from the POGO (1965–1971) and Magsat (1979–1980) satellites. The CM4 model covers the period 1962–2002 and includes similar observatory and satellite data as well as data from the recent Ørsted (since 1999) and CHAMP (since 2000) satellites. CHAOS-2 is the most recent model of the three and includes ten years of Ørsted data (March 1999 – March 2009), almost nine years of CHAMP data (August 2000 – March 2009), and 4 years of SAC-C data (January 2001 – December 2004); it also includes observatory data from 1997 to 2006. In this paper, we use the CHAOS-2s version of CHAOS-2, either truncated at degree 20 (Earth's surface) or degree 13 (core surface).

[8] There is good agreement between the drift obtained from directly observed NMP positions and that obtained from NMP positions derived from global models. All model positions lie within the error bars of the observed positions, except the 1973 position obtained from *gufm1*, which lies 59.1 km from the observed position, and the 1973 CM4 position, which lies 70.4 km from the observed position. This suggests that the positional uncertainty might very well be almost constant over the 20th century, as hypothesized when assigning the same error bars to all observations in Figure 1.

[9] The plot of the drift shown in Figure 1 can be divided into four distinct sections.

[10] 1. From 1831 to 1904, the drift is nearly zero. The distance between the 1831 and 1904 observed positions is within the error bar assigned to these positions. The increasing (unsigned) distance from 1831 to about 1860 in the *gufm1* curve actually corresponds to a period of southward drift [Newitt *et al.*, 2002], after which the NMP reversed direction and started to move northward. The total distance covered in the southward direction is, however,

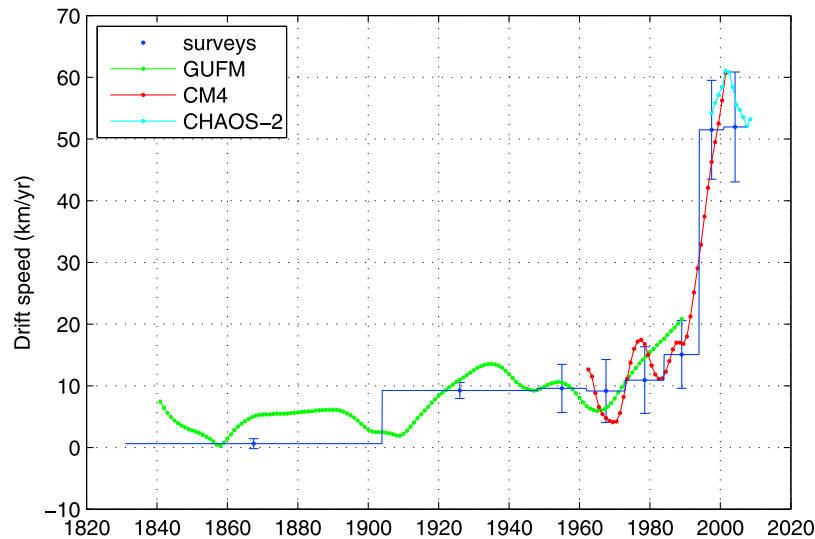


**Figure 2.** Average drift speeds (in km/yr) from the observed NMP positions (in blue), represented as stairs delimited by the observation dates, and with estimated error bars. Drift speed (in km/yr) of the NMP positions calculated from the *gufm1* (in green), CM4 (in red) and CHAOS-2 (in light blue) geomagnetic models.

small (less than 200 km) and one should keep in mind that 19th century data used in *gufm1* are probably not as good as 20th century data, due to the very limited number of reliable magnetic observatories before 1900 [Jackson *et al.*, 2000].

[11] 2. From 1904 to 1984, the observed NMP positions show an almost linear increase in distance with time, at a speed of around 10 km/yr. There are small oscillations in the model curves that cannot be confirmed by direct observations since the time intervals between successive observations are too large.

[12] 3. From 1984 to 2001, both direct observation and the CM4 model show a large increase in drift rate, from about 10 km/yr to 50 km/yr.

[13] 4. From 2001 to the present, the drift velocity has remained high (about 50 km/yr) but the acceleration has been close to zero.

[14] The same four phases are visible in Figure 2, which shows the NMP drift speed versus time. In Figure 2, the average drift speeds from the observed NMP positions are represented as stairs delimited by the observation dates in order not to confuse them with instantaneous drift speeds obtained from time varying spherical harmonics models. Assuming that the positional error for all observed positions is 40 km (see above), we calculated error bars on average drift speeds by dividing the error in the distance between points ( $40\sqrt{2} = 56$  km) by the number of years between observations. The increase of these error bars in recent years simply reflects more frequent measurements.

[15] Taking the time derivative of the drift enhances the small oscillations in the *gufm1* and CM4 models. The CM4 curve displays the 1969 and 1978 local extrema noted by Mandeia and Dormy [2003], which they attribute to geomagnetic jerks that occurred at the same time as the extrema. These extrema are absent from the *gufm1* curve, possibly due to the use of a less sophisticated modeling technique than CM4 (which co-estimates internal and external fields). Note that Mandeia and Dormy [2003] (and later Olsen and

Mandeia [2007a]) actually found 1969 and 1978 extrema in their *gufm1* curve, a result we were not able to reproduce. Average drift speeds obtained from surveys seem to be in better agreement with the CM4 model than with *gufm1* between 1983 and 1994, but do not discriminate between these models for earlier time intervals (1962–1973 and 1973–1984). The most prominent feature in Figure 2 is the dramatic increase in drift speed that took place in the 1990s, from 15 km/yr to a little more than 50 km/yr according to surveyed positions, and even 60 km/yr according to the CM4 and CHAOS-2 models. This acceleration is well above the error bars on average drift speeds obtained from the observed positions. The CM4 and CHAOS-2 models make it possible to determine that the period of acceleration began in 1989 and ended in 2002. It is worth noting that CM4 is based on satellite data providing a good spatial coverage before (MAGSAT) and after (Ørsted and CHAMP) the 1990s. Furthermore, the fact that the pole acceleration is reproduced by the internal spherical harmonic coefficients clearly points at a core origin of this phenomenon. The steep acceleration is followed by a leveling off of the drift speed of the observed NMP positions, and even a slight decrease in the drift speed of NMP positions determined from the CHAOS-2 model after 2002.5.

### 3. NMP Drift Speed and Secular Variation in the North Polar Region

[16] In what follows, we focus on the time interval 1962–2009 in order to identify the cause of the sudden acceleration of the NMP in the 1990s. Assuming that the CM4 model is more accurate than the *gufm1* model in this time interval, all subsequent calculations are based on CM4 and CHAOS-2, as well as the direct observations.

[17] We first investigate the geomagnetic secular variation at nearby magnetic observatories. The Resolute Bay (IAGA code RES) and Qaanaaq (Thule, IAGA code THL) obser-

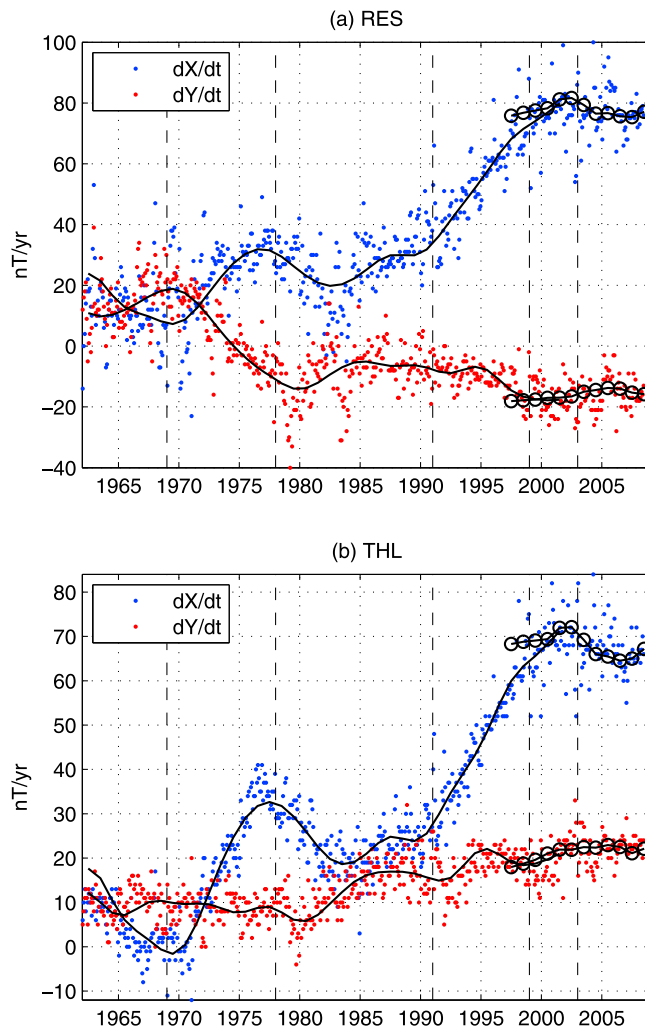


**Figure 3.** Annual differences (in nT/yr) of the  $X$  (blue) and  $Y$  (red) components at (a) RES and (b) THL observatories. The annual differences calculated from the CM4 (black line) and the CHAOS-2 (black line with circles) geomagnetic models are also shown. Dates of geomagnetic jerks are shown by black dashed lines.

observatories are the two closest to the NMP. Between 1962 and 2009, the distance from the NMP to RES ranged from 164 km to 1235 km, and the distance from the NMP to THL ranged from 801 km to 1195 km. The  $X$  and  $Y$  components of the secular variation at each observatory are displayed in Figure 3. The plotted values are annual differences of observatory monthly means (from all day values), calculated by taking the difference between monthly means at  $t+6$  months and  $t-6$  months, in order to remove seasonal variations in the data. On the same graphs, the annual differences of core field values calculated from the CM4 and CHAOS-2 models are also shown. We note that there is a very good agreement between the observed annual differences and those calculated from the models. The data from both observatories reveal an abrupt increase in  $dX/dt$  between 1989 and 2002, followed by a leveling off and even a slight decrease. The total change in secular variation between 1989

and 2002 is similar at both observatories, reaching about 50 nT/yr at RES and 45 nT/yr at THL. (Note that here, as in the rest of the paper, “change in secular variation” refers to a finite change in the secular variation between two epochs, expressed in nT/yr, and not the time derivative of the secular variation, expressed in nT/yr<sup>2</sup>.) These values are much larger than the error bars on annual differences, which range from 10 to 30 nT/yr (approximately). The  $Y$  component does not show a similar change in secular variation.

[18] Also shown in Figure 3 are the dates of known geomagnetic jerks over the 1962–2009 time interval: 1969, 1978, 1991, 1999 and 2003 [Macmillan, 1996; Mandaia et al., 2000; Olsen and Mandaia, 2007b]. The first two jerks are clearly visible in the  $X$  and  $Y$  components at RES, in  $X$  only at THL, with time delays smaller than two years. However, the abrupt increase in  $dX/dt$  in the 1990s started two years before the 1991 jerk; it finished three years after the 1999 jerk and one year before the 2003 jerk. Therefore the relationship between these three jerks and the 1990s large change in the secular variation is not straightforward.

[19] Compared to earlier episodes of increasing/decreasing secular variation at RES and THL, the change in  $dX/dt$  over the time interval 1989–2002 is unusually large; the second largest change in  $dX/dt$  at THL, which was only about 30 nT/yr, occurred between the 1969 and 1978 geomagnetic jerks; earlier episodes at THL were even weaker. The change is also very large compared to changes in secular variation over the same 1989–2002 time interval in other regions of the Earth’s surface, as can be seen in Figure 4. There is a maximum of about 50 nT/yr in the Canadian Arctic, and another one in Eastern Siberia. Everywhere else, the secular variation change is less than 30 nT/yr.

[20] To understand the possible connection between the sudden increase in the NMP drift speed and the simultaneous, unusually large Canadian Arctic secular variation

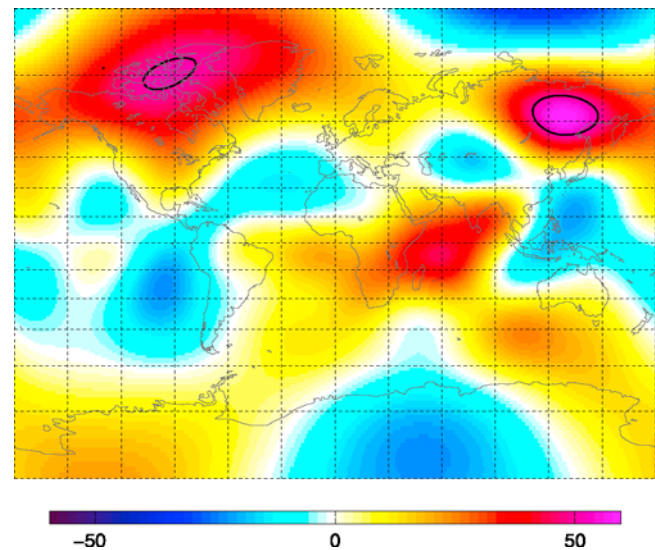


**Figure 4.** Change in secular variation (in nT/yr) of the  $X$  component at the Earth’s surface between 1989 and 2002, computed from the CM4 geomagnetic model. The solid black curves are 50 nT/yr contour lines.

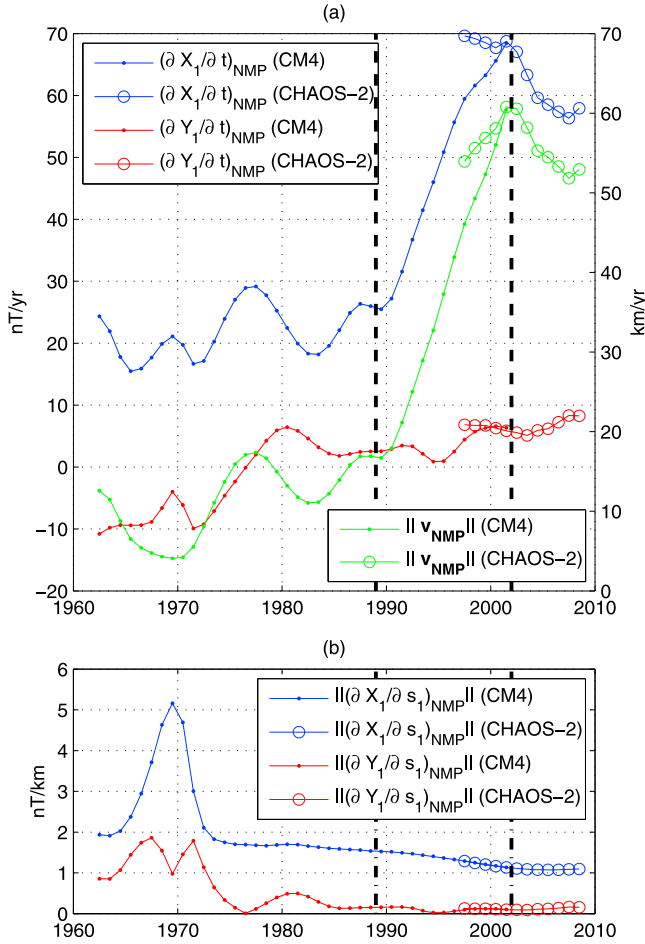


**Figure 5.** (a) Temporal evolution of the NMP's drift speed (green curves, in km/yr) given by the CM4 (small dots) and CHAOS-2 (circles) models. Also shown, the temporal evolution of the secular variation components at the NMP along  $(\partial X_1/\partial t)_{NMP}$ , blue curves) and perpendicular  $(\partial Y_1/\partial t)_{NMP}$ , red curves) to the NMP drift direction, from CM4 (small dots) and CHAOS-2 (circles). (b) Temporal evolution of the local gradient in the direction of the NMP's drift. The  $X_1$  ( $(\partial X_1/\partial s_1)_{NMP}$ ) component (in blue) and  $Y_1$  ( $(\partial Y_1/\partial s_1)_{NMP}$ ) component (in red) are computed at the NMP position from CM4 (small dots) and CHAOS-2 (circles). Units in nT/km. Dates of the beginning (1989) and end (2002) of the 1990s acceleration episode are shown by dashed or dash-dotted black lines.

increase, we now formally relate the two quantities. We first introduce magnetic field components parallel ( $X_1$ ) and perpendicular ( $Y_1$ ) to the NMP drift direction

$$X_1 = \mathbf{B} \cdot \frac{\mathbf{V}_{NMP}}{\|\mathbf{V}_{NMP}\|}, \quad (1)$$

$$Y_1 = \mathbf{B} \cdot \left( -\hat{\mathbf{r}} \times \frac{\mathbf{V}_{NMP}}{\|\mathbf{V}_{NMP}\|} \right), \quad (2)$$

where  $\mathbf{B}$  is the magnetic field,  $\mathbf{V}_{NMP}$  the NMP drift velocity and  $\hat{\mathbf{r}}$  the unit vector directed radially outward. At the NMP,

defined as the location where  $X = Y = 0$ , we have  $X_1 = Y_1 = 0$  at all times. Hence,

$$\frac{\partial X_1}{\partial t} \Big|_{NMP} + \mathbf{V}_{NMP} \cdot \nabla_H X_1 \Big|_{NMP} = 0, \quad (3)$$

where  $\nabla_H = \nabla - \hat{\mathbf{r}}\partial_r$ , and the same for  $Y_1$ , yielding

$$\|\mathbf{V}_{NMP}\| = - \frac{1}{\frac{\partial X_1}{\partial s_1} \Big|_{NMP}} \frac{\partial X_1}{\partial t} \Big|_{NMP}, \quad (4)$$

$$= - \frac{1}{\frac{\partial Y_1}{\partial s_1} \Big|_{NMP}} \frac{\partial Y_1}{\partial t} \Big|_{NMP}, \quad (5)$$

where  $s_1$  is the curvilinear coordinate along the NMP drift trajectory. (Note that, since this drift is almost rectilinear,  $\frac{\partial X_1}{\partial t} \Big|_{NMP}$  and  $\frac{\partial Y_1}{\partial t} \Big|_{NMP}$  are projections of the NMP secular variation along directions that remain the same during the period of interest.)

[21] Figure 5 shows the time evolution of the five quantities involved in Equations 4 and 5. The variations in the NMP drift speed generally follow the variations in  $\frac{\partial X_1}{\partial t} \Big|_{NMP}$ , except around 1970 (Figure 5a). From 1989 to 2002, about 75 percent of the increase in the drift speed of the NMP (from about 15 km/yr to about 60 km/yr, i.e., a factor of four) can be attributed to the local increase in secular variation of the  $X_1$  component (from 25 nT/yr to about 70 nT/yr, i.e., a factor of three). The remaining 25 percent of the increase is due to the local decrease in the  $\frac{\partial X_1}{\partial s_1} \Big|_{NMP}$  gradient, from about 1.5 nT/km to 1 nT/km (Figure 5b). After 2002, there is no further change in the gradient and the observed decrease in the NMP drift speed is caused entirely by a corresponding decrease in  $\frac{\partial X_1}{\partial t} \Big|_{NMP}$ . The  $Y_1$  component is less useful in interpreting the 1990s acceleration episode due to the lack of correlation between its secular variation and the NMP acceleration. Still, its secular variation increases, although less than in the case of  $X_1$ , and its gradient along the NMP trajectory decreases.

[22] We conclude that the unusually large increase in the rate of drift of the NMP over the time interval 1989–2002 is primarily a manifestation of an unusually large increase in the secular variation of the horizontal magnetic field in the NMP area, particularly in the  $\frac{\partial X_1}{\partial t} \Big|_{NMP}$  component parallel to the NMP drift trajectory.

## 4. Identifying the Core Processes Responsible for the NMP's Acceleration

### 4.1. Change in Secular Variation at the Core Surface From 1989 to 2002

[23] Assuming that the mantle is perfectly insulating, the Earth's magnetic field satisfies Laplace's equation between the core-mantle boundary (CMB) and the Earth's surface. It follows that spherical harmonic models of the core field can be downward continued to the CMB. Moreover, the radial magnetic field is continuous through the CMB. Using these properties, we used the CM4 model to calculate the total

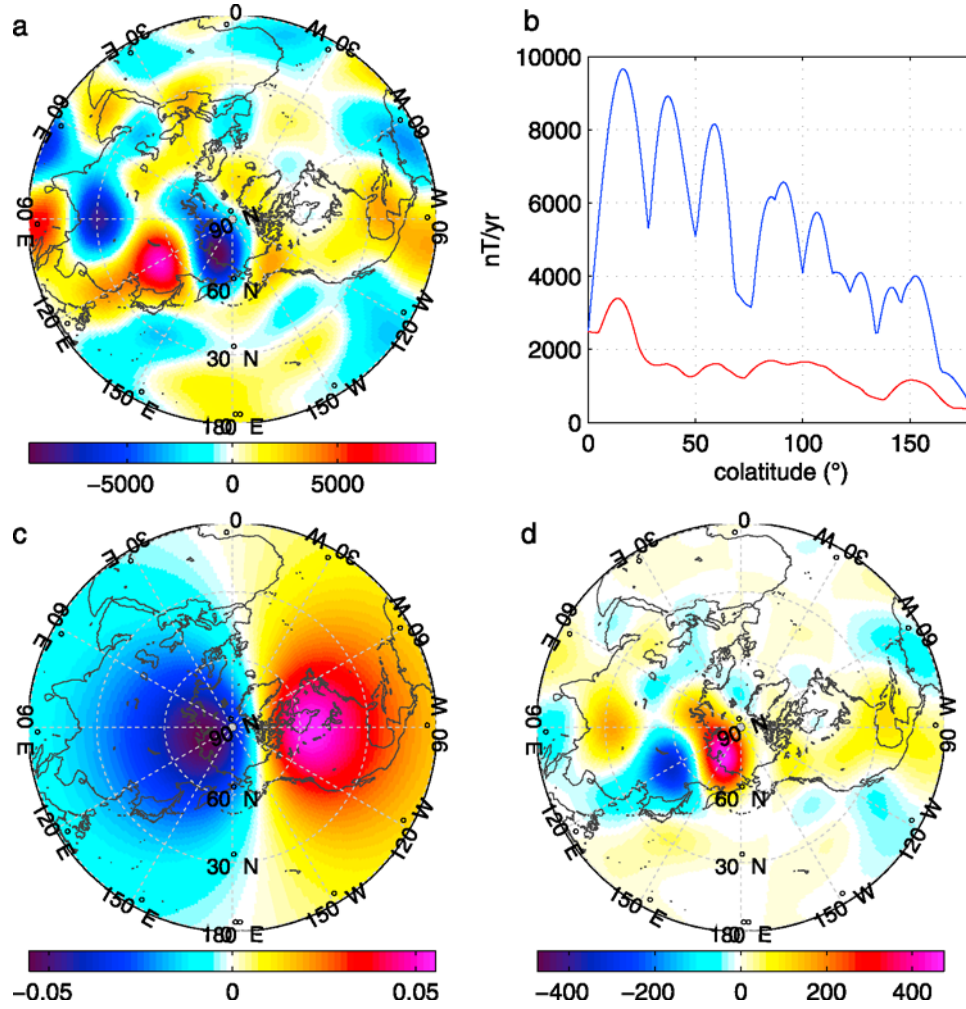


**Figure 6.** Polar views (between colatitudes  $0^\circ$  and  $90^\circ$ ) of (a) the total radial secular variation change at the core surface  $\int_{t_1}^{t_2} \frac{\partial^2 B_r}{\partial t^2} dt$  (in nT/yr), where  $t_1 = 1989$ ,  $t_2 = 2002$  and  $B_r$  is calculated from CM4; (c) the Green's function  $G_{X_1}(\mathbf{r}, \hat{\mathbf{s}})$  for  $\mathbf{r}$  at the 1995.5 NMP (no unit); (d) the integral  $\int_{t_1}^{t_2} G_{X_1}(\mathbf{r}, \hat{\mathbf{s}}) \frac{\partial^2 B_r}{\partial t^2}(\hat{\mathbf{s}}, t) dt$  (in nT/yr), where  $\mathbf{r}$  is at the NMP. (b) Maximum (blue curve) and mean (red curve) of the absolute total secular variation change  $|\int_{t_1}^{t_2} \frac{\partial^2 B_r}{\partial t^2} dt|$  (in nT/yr) at the core surface as a function of the colatitude. See text for definitions and notations.

change in the secular variation of the radial magnetic field at the core surface between 1989 and 2002. As shown in Figure 6a, this change reaches almost 10000 nT/yr in two areas: within a negative patch centered under New Siberian Islands (near  $75^\circ\text{N}$ ,  $150^\circ\text{E}$ ), and within a positive patch centered under north-eastern China (near  $50^\circ\text{N}$ ,  $120^\circ\text{E}$ ). It is smaller everywhere else, both in the northern and southern (not shown) hemispheres.

[24] The predominance of the patches below New Siberian Islands and north-eastern China leads to the two largest peaks that can be seen in Figure 6b, which shows the maximum and mean total secular variation change for each latitude band at the core surface. Interestingly, both curves show that the SV change at the CMB decreases steadily from the north polar region to the south polar region. The total secular variation change from 1989 to 2002 is hemispherically asymmetrical, being much larger in the northern hemisphere. Not surprisingly, this asymmetry is also to be seen in the secular variation change in the  $X$  component at

the Earth's surface (Figure 4). Could the extremely large secular variation changes at the core surface under New Siberian Islands and north-eastern China, as shown in Figure 6a, be responsible for the large change in  $\left. \frac{\partial X_1}{\partial t} \right|_{NMP}$  that caused the NMP to accelerate between 1989 and 2002?

#### 4.2. Green's Function Analysis

[25] To address this question, we need to express  $X_1$  at any point  $\mathbf{r}$  at the Earth's surface in terms of the radial component  $B_r$  at the CMB. This can be done with the help of a Green's function for the Neumann problem [Gubbins and Roberts, 1983; Constable et al., 1993]. Using Equations (2)–(5) from [Constable et al., 1993], which apply to any horizontal component,  $X_1(\mathbf{r}, t)$  can be related to  $B_r(\hat{\mathbf{s}}, t)$  through

$$X_1(\mathbf{r}, t) = \int_S G_{X_1}(\mathbf{r}, \hat{\mathbf{s}}) B_r(\hat{\mathbf{s}}, t) d^2 \hat{\mathbf{s}} \quad (6)$$

where

$$G_{X_1}(\mathbf{r}, \hat{\mathbf{s}}) = -\frac{1}{4\pi} \left[ \frac{1 - \rho^2 + 2R}{R^3 T} \right] \rho^3 \hat{\mathbf{s}} \cdot \hat{\mathbf{x}}_1 \quad (7)$$

and

$$\rho = \frac{c}{r}, \quad \mu = \hat{\mathbf{r}} \cdot \hat{\mathbf{s}} \quad (8)$$

$$R = \sqrt{1 - 2\mu\rho + \rho^2}, \quad T = 1 + R - \mu\rho. \quad (9)$$

Here  $c$  is the core radius,  $\hat{\mathbf{r}}$  is the unit vector in the direction of  $\mathbf{r}$  at the location where  $X_1(\mathbf{r}, t)$  is defined,  $\hat{\mathbf{x}}_1$  is the unit vector in the  $X_1$  direction, and  $\hat{\mathbf{s}}$  is a radial unit vector defining the location at the core surface over which the integral runs.

[26] The total secular variation change in the  $X_1$  component at the NMP may then be expressed as the sum of the secular variation due to the field change and that due to the NMP movement

$$\begin{aligned} \left. \frac{\partial X_1}{\partial t} \right|_{NMP} (t_2) - \left. \frac{\partial X_1}{\partial t} \right|_{NMP} (t_1) &= \int_{t_1}^{t_2} \left\{ \left. \frac{\partial^2 X_1}{\partial t^2} \right|_{NMP} \right. \\ &\quad \left. + (\mathbf{V}_{NMP} \cdot \nabla_H) \left. \frac{\partial X_1}{\partial t} \right|_{NMP} \right\} dt \\ &= \int_S \left\{ \int_{t_1}^{t_2} G_{X_1} \frac{\partial^2 B_r}{\partial t^2} dt \right\} d^2 \hat{\mathbf{s}} \\ &\quad + \int_S \left\{ \int_{t_1}^{t_2} \|\mathbf{V}_{NMP}\| \frac{\partial G_{X_1}}{\partial s_1} \frac{\partial B_r}{\partial t} dt \right\} d^2 \hat{\mathbf{s}}. \end{aligned} \quad (10)$$

Taking  $t_1 = 1989$  and  $t_2 = 2002$ , we obtain 50.8 nT/yr and  $-7.8$  nT/yr for the first and second integrals of the RHS of Equation (10), respectively. This shows that the main contributor to the observed change in the secular variation  $\left. \frac{\partial X_1}{\partial t} \right|_{NMP}$  along the NMP drift trajectory at the Earth's surface is the integral

$$I = \int_S \left\{ \int_{t_1}^{t_2} G_{X_1} \frac{\partial^2 B_r}{\partial t^2} dt \right\} d^2 \hat{\mathbf{s}}. \quad (11)$$

[27] The Green's function  $G_{X_1}(\mathbf{r}, \hat{\mathbf{s}})$  for  $\mathbf{r}$  at the 1995.5 NMP is mapped at the core surface (northern hemisphere) in Figure 6c. Its product with the total change in the secular variation of the radial component over  $[t_1, t_2] = [1989, 2002]$  (mapped in Figure 6a) is shown in Figure 6d using the same polar view between colatitudes  $0^\circ$  and  $90^\circ$ . We have numerically checked that

$$\int_{t_1}^{t_2} G_{X_1} \frac{\partial^2 B_r}{\partial t^2} dt \approx G_{X_1} \int_{t_1}^{t_2} \frac{\partial^2 B_r}{\partial t^2} dt, \quad (12)$$

which it should be, due to the negligible variation of  $G_{X_1}$  over  $[t_1, t_2]$ . This quantity and the Green's function  $G_{X_1}$  are not plotted for the southern hemisphere because contributions from this part of the core surface to the integral  $I$  are negligible. Figures 6c and 6d show that the Green's function dampens most contributions to  $I$  except the large negative radial secular variation change observed under the New

Siberian Islands. Even the positive radial secular variation change observed under north-eastern China is significantly damped. We conclude that the main cause of the NMP's acceleration between 1989 and 2002 is the presence of an area of large, negative change in the secular variation of  $B_r$  under the New Siberian Islands. The effect of this change is only partly offset by a positive secular variation change in  $B_r$  under north-eastern China, to which the NMP drift was less sensitive.

### 4.3. Interpretation in Terms of Core Processes

#### 4.3.1. Magnetic Upwelling

[28] The large secular variation decrease observed under the New Siberian Islands in Figure 6a may also be visualized by mapping the radial secular variation at the core surface in the north polar region in 1989 and 2002 (Figures 7a and 7b). At both epochs, the map is dominated by the same pair of patches of opposite polarities: a positive patch located under the New Siberia Islands and a negative patch located under the Bering Strait. From 1989 to 2002, the secular variation under both patches decreased markedly in algebraic value, as observed in Figure 6a.

[29] The origin of the observed pair of secular variation patches might be the upwelling of a thermal-wind driven plume from the inner-core boundary to the CMB, as observed by *Aubert et al.* [2008] in their numerical simulations. Such thermal-wind driven plumes can rise within the cylinder tangent to the inner core (hereafter referred to as the "tangent cylinder"), producing what *Aubert et al.* [2008] define as "polar magnetic upwelling" and leading to the formation of pairs of CMB radial flux patches having opposite polarities (see their Figure 8). During this process, the radial secular variation is also expected to map as a pair of oppositely directed patches at the core surface, even before a reversed flux patch forms at the core surface. As can be seen in Figures 7a and 7b, the New Siberia Islands/Bering Strait pair of secular variation patches lies across the trace at the core surface of the tangent cylinder, in good agreement with this scenario. Also, Figures 7c and 7d show that a new reversed flux patch seems to have emerged from the core under the New Siberian Islands during the 1990s. This observation is confirmed by the CHAOS-2 model (not shown), which was calculated from an independent data set. The second flux patch of the pair would then be the negative patch under the Bering Strait, which seems to have strengthened between 1989 and 2002. Based on this scenario, the decrease in secular variation which led to the acceleration of the NMP in the 1990s could be attributed to a slowdown in the New Siberian Islands/Bering Strait upwelling, possibly due to the deceleration of the rising plume.

[30] Could the upwelling mechanism explain other structures in the radial field and secular variation near the tangent cylinder? It is interesting to note that there are actually two other pairs of secular variation patches of opposite polarity in the vicinity of the tangent cylinder: one located under the Canadian Arctic and eastern Greenland; the other one, much weaker, located under the Greenland Sea and Novaya Zemlya (Figures 7a and 7b). The first pair is related to the large, reversed flux patch centered under the Arctic Ocean (hereafter referred to as the North Pole patch); the second pair is related to the smaller reversed flux patch centered under the Barents Sea (Figures 7c and 7d). The flux through



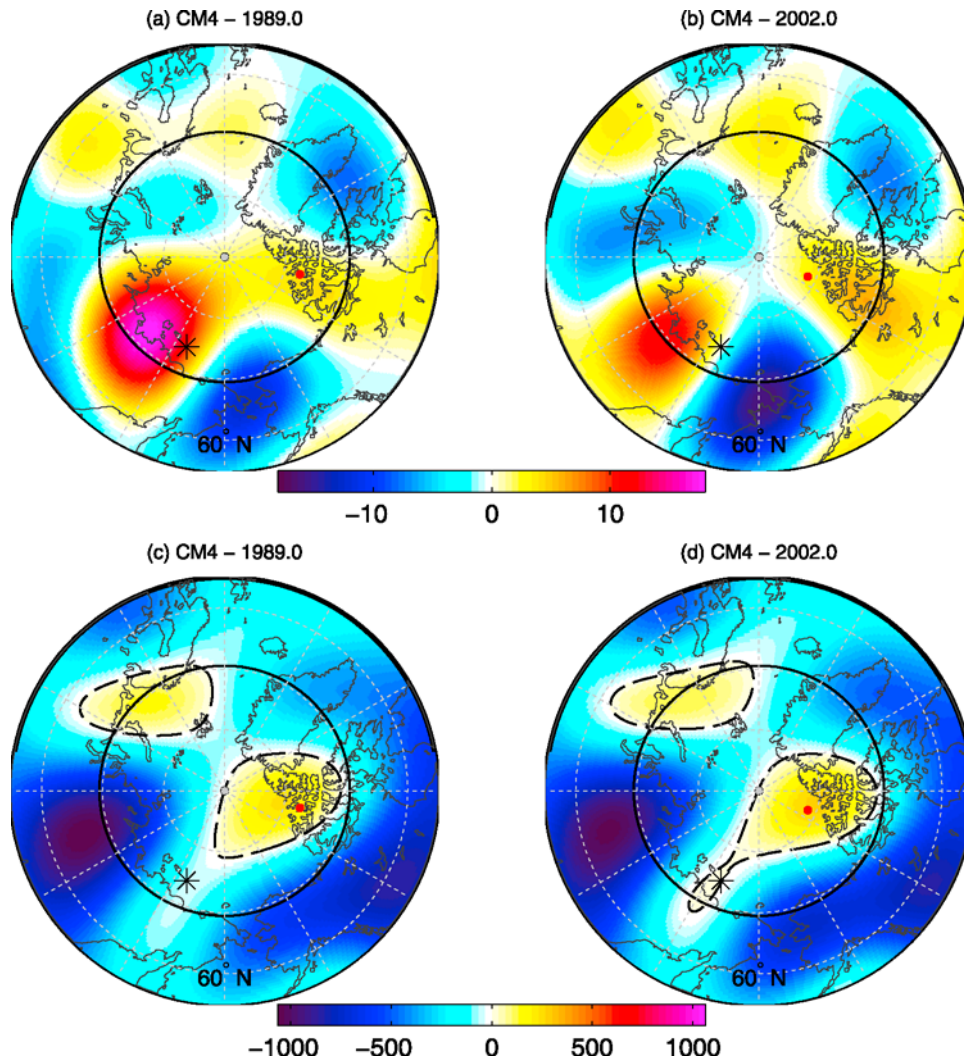


**Figure 7.** Polar views (from colatitude  $0^\circ$  to  $55^\circ$ ) of the radial secular variation (in  $\mu\text{T}/\text{yr}$ ) at the core surface from the CM4 model in (a) 1989 and (b) 2002. (c and d) Same for the radial magnetic field (in  $\mu\text{T}$ ) at the core surface; the  $B_r = 0$  level curves are represented as dashed black curves. The NMP (at the Earth's surface) is represented by a red dot. The location of the maximum change in total secular variation (radial component) at the core surface over the time interval 1989 to 2002 is represented by a black star. The black solid circle represents the trace at the core surface of the cylinder tangent to the inner core.

the North Pole patch increased over the 1989–2002 time interval, while the flux through the Barents Sea patch remained almost constant over the same time interval. This can also be seen in Figure 8, where we have plotted the time evolution of fluxes (computed using the method of *Shure et al.* [1982]) through the North Pole and Barents Sea patches since 1840. (Note that the differences between absolute flux values from different models at some epochs are due to differences in model regularizations; what matters is the time variation of the fluxes, which is in good agreement from one model to the next.) These observations are in good agreement with the magnetic upwelling scenario. One could even speculate that the three identified magnetic upwellings might be at three different stages of their evolution: the New Siberian Islands/Bering Strait upwelling would be at an initial stage where the reversed flux patch would just be emerging from the core; the Canadian Arctic/

eastern Greenland upwelling would be at an intermediate stage where the reversed flux patch would be formed and still growing; the Greenland Sea/Novaya Zemlya upwelling would be at a later stage where the growth has stopped.

#### 4.3.2. Magnetic Diffusion

[31] The magnetic upwelling observed by *Aubert et al.* [2008] in their simulation led to the expulsion of magnetic flux from the core, a process involving a significant amount of magnetic diffusion, hence a local failure of the frozen-flux assumption [*Roberts and Scott, 1965*]. On the observational side, magnetic diffusion is expected to be detected as local violations of the following necessary conditions for the frozen flux hypothesis [*Backus, 1968*]: (1) the magnetic flux through each patch delimited by a  $B_r = 0$  curve (i.e., reversed flux patch) should remain constant; (2) the secular variation at critical points where  $B_r = 0$  and  $\|\nabla_H B_r\| = 0$  (i.e., where two  $B_r = 0$  curves cross each other) should be zero.

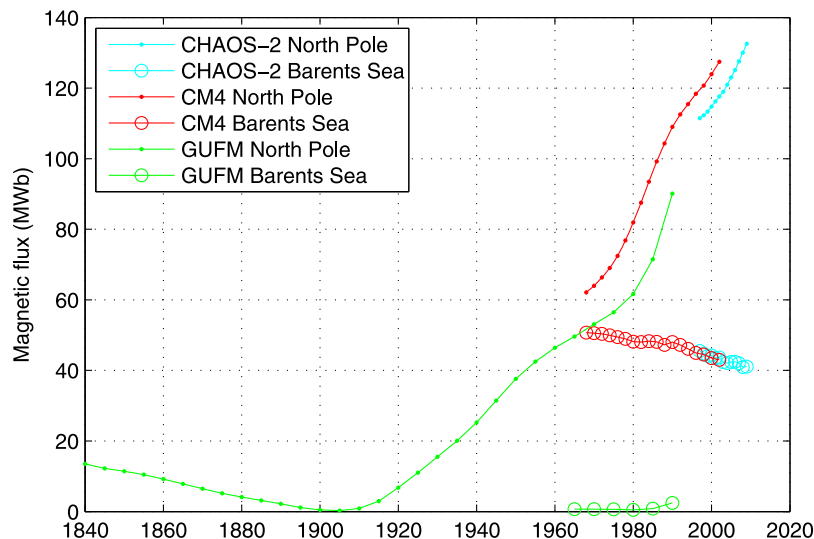


**Figure 8.** Magnetic flux (in MWb) through the North Pole and Barents Sea reversed flux patches as a function of time, computed from three geomagnetic models: *gufm1* (in green), CM4 (in red) and CHAOS-2 (in light blue).

Figures 7c and 7d and 8 suggest a violation of the first condition in the North Pole reversed flux patch, as the flux through this patch increased by about 20% from 107 MWb to 127 MWb between 1989 and 2002. According to the *gufm1* model, the flux expulsion may have started as early as the 1900s and its rate remained roughly constant at about 8 MWb/yr until 1980, after which it increased. By contrast, the flux through the Barents Sea patch remained almost constant after it separated from the North Pole patch in the 1960s. Figures 7c and 7d also suggest a possible violation of type (2) under New Siberian Islands. The emergence of a new reversed flux patch in this area necessarily lead to the temporary appearance of a critical point, either as an isolated point if the patch emerged independently from the North Pole patch, or as a saddle point if it separated from that patch; according to CM4, it seems to have been an isolated point around 1996 (not shown).

[32] How much diffusion could then be involved in the emergence of the New Siberian Islands reversed flux patch? The key parameter here is the amount of secular variation near the critical point. Let us write the radial component of the induction equation at the top of the core [Gubbins and Roberts, 1987]

$$\frac{\partial B_r}{\partial t} = -\nabla_H \cdot (\mathbf{u}B_r) + \eta \nabla^2 B_r, \quad (13)$$

where  $\nabla_H = \nabla - \mathbf{n}\partial_r$ ,  $\mathbf{n}$  being the unit radial outward vector,  $\mathbf{u}$  is the fluid velocity just below the thin viscous boundary layer at the top of the core, and  $\eta$  is the magnetic diffusivity in the core. At and near a critical point  $C$ , we have a purely diffusive secular variation

$$\left(\frac{\partial B_r}{\partial t}\right)_C \approx (\eta \nabla^2 B_r)_C. \quad (14)$$

Note that this equation is the limit when the  $B_r = 0$  curve reduces to a point of Eq. (5') of Hulot and Chulliat [2003].

According to CM4, the secular variation in the critical point area was about 5000 nT/yr in 1996 and regularly decreased from about 10000 nT/yr in 1989 to about zero in 2002. This represents a large amount of secular variation compared to other regions of the core surface (see Figures 7a and 7b), hence a significant amount of magnetic diffusion.

[33] A similar conclusion is reached if one assumes that the frozen-flux assumption holds in the New Siberian Islands area and applies local methods to calculate core surface flows from secular variation [Chulliat and Hulot, 2000; Chulliat, 2004]. Such techniques rely on the tangentially geostrophic hypothesis [Le Mouél, 1984], which is thought to be very well satisfied along the  $B_r = 0$  level curves (where the Lorentz force vanishes) and in their vicinity. In the polar region, where  $\cos \theta \approx 1$ , one has the following simplified expression for the component of the flow perpendicular to the local level curve of  $B_r$  [Chulliat, 2004]

$$\mathbf{u}_\pi = -\frac{1}{\cos \theta \|\nabla_H B_r\|} \frac{\partial B_r / \partial t}{\pi}, \quad (15)$$

where  $\pi = \nabla_H B_r / \|\nabla_H B_r\|$  is the unit vector normal to the level curve of  $B_r$ . (The flow along that level curve is left unconstrained by the secular variation as it belongs to the null space of the problem.) Applying this formula to the point on the core surface where the secular variation change is maximum over 1989–2002 (marked as a black star in Figures 7a–7d), we find that  $\|\mathbf{u}_\pi\|$  at this point varies from 34.9 km/yr in 1989 to 1.52 km/yr in 2002, with a peak at 221.1 km/yr in 1996. Even larger and more unlikely speeds would be found at points nearer the critical point, thus supporting the previous conclusion that magnetic diffusion is likely to be needed to explain the observed secular variation.

[34] Could this apparent failure of the frozen-flux assumption result from a lack of resolution of the CM4 model? The unobserved small scale core field (i.e., degrees of the spherical harmonic expansion greater than 14) is likely to modify the exact shape of the  $B_r = 0$  curve under

New Siberian Islands, and displace the location of the critical point  $C$ . Likewise unobserved small scale secular variation must contribute to the secular variation at this critical point  $C$ . As a result, we cannot dismiss the possibility that such small scales could reconcile the location of the critical point with a zero value of the secular variation. It nevertheless remains that with its accessible resolution CM4 clearly suggests the creation of a New Siberian Island reversed flux patch. This patch is also seen in the CHAOS-2 model (not shown), which was calculated from an independent data set and using a different method. Moreover, the non-zero secular variation of  $B_r$  in this area for at least part of the time interval under consideration is probably a very robust feature, as it is required to explain the NMP's acceleration (which results precisely from a large change in the  $B_r$  secular variation). The occurrence of magnetic flux expulsion from the core in this area, though not proven, simply provides a straightforward explanation for all those observations.

## 5. Discussion

[35] In the previous two sections we have shown that the origin of the unusually large acceleration in the motion of the NMP that occurred during the 1990s is a large localized change in secular variation at the core surface under New Siberian Islands. The NMP happened to be at an optimal location to sense that event (via the Green's function). This change has been attributed to an episode of magnetic flux expulsion under the New Siberian Islands, close to the Siberian tip of the North Pole reversed flux patch. We now discuss these results in the context of previous studies of NMP drift and magnetic diffusion in the core.

[36] *Olsen and Manda* [2007a] recently conjectured that the growth and poleward motion of the North Pole reversed flux patch could be responsible for the northward drift of the NMP. Our Green's function analysis shows that the role played by the North Pole reversed flux patch in causing the acceleration of the NMP is not the one suggested by these authors. Both Green's functions are zero near the center of the reversed flux patch, precisely because it is located right under the NMP. Therefore any growth of the magnetic flux in this area has a negligible effect on the horizontal magnetic field near the NMP. The effect of the reversed flux patch on the NMP's drift speed is more subtle, as it is only an episode of localized growth near the Siberian side of the patch that caused the acceleration in drift during the 1990s, not the growth of the entire patch.

[37] What is the validity of our interpretation in terms of magnetic diffusion? Many attempts have been made in the past to test the frozen-flux assumption, with mixed results depending on the method used [e.g., *Wardinski and Holme*, 2006; *Jackson et al.*, 2007, and references therein]. A proper test requires a rigorous error analysis, which would go beyond the scope of the present paper. However, theoretical works [*Allan and Bullard*, 1966; *Bloxham*, 1986; *Gubbins*, 2007] as well as recent numerical simulations of the geodynamo [e.g., *Amit et al.*, 2007; *Aubert et al.*, 2008] strongly suggest the existence of regions of the core surface where the magnetic field is being expelled from the core via a diffusive process. Recently, *Chulliat and Olsen* [2010] used high-precision satellite magnetic data and advanced global models of the external field to construct core field models

that incorporated the Backus constraints. Using these models they were able to detect traces of magnetic diffusion under St Helena Island over the time interval 1980–2005 thus supporting theoretical results. They also detected some magnetic diffusion within the North Pole reversed flux patch over the same time interval, but this result was found to be less robust. This does not contradict the interpretation made in the present paper, as most of the diffusion involved in the emergence of the New Siberian Islands reversed flux patch would have occurred before this patch became visible at the core surface and therefore testable using Backus constraints.

[38] According to some core flow models, there is a westward polar vortex around the North Pole [*Pais and Hulot*, 2000; *Hulot et al.*, 2002; *Holme and Olsen*, 2006], a feature first noted by *Olson and Aurnou* [1999] from a direct inspection of the  $B_r = 0$  curves in this area. Looking at Figures 7c and 7d, one can actually notice a small clockwise rotation of the  $B_r = 0$  curves between 1989 and 2002, in good agreement with such models. However, the simple flow calculation presented in section 4.3.2 shows that this rotation cannot explain the observed secular variation change under New Siberian Islands and that a much larger, unrealistic, flow would be needed. Rotation and magnetic flux expulsion are not incompatible and can coexist, as can be seen from Figures 7a and 7b, which show the secular variation patches also seem to rotate in the same direction as the field structures.

[39] *Newitt et al.* [2002] and *Manda and Dormy* [2003] invoked possible relationships between geomagnetic jerks and the NMP drift speed, based on the timing of variations in the NMP's drift speed before the 1990s. Our results show that the 1990s acceleration phase started in 1989 and ended in 2002, i.e., two years before the 1991 jerk and three years after the 1999 jerk, respectively. In fact, the same lack of synchronization is observed at the two nearby observatories, RES and THL. More problematic in our view is that the jerk phenomenon as it is usually defined (a local change of sign of the secular variation trend, observed globally) does not account for the unusually large increase of  $dX_1/dt$  over the 1990s. Instead, we showed that the acceleration of the NMP in the 1990s was caused by a local phenomenon, amplified by some geometrical effects (i.e., the Green's function). Whether this local phenomenon could be related in some way to jerks remains an open question. Properly addressing it would require a satisfactory interpretation of geomagnetic jerks in terms of core dynamics, which we presently do not have.

[40] Finally, an interesting question is whether the direction and speed of the NMP's drift can be forecast. *Olsen and Manda* [2007a] recently speculated that "one may expect decreasing velocity once [the NMP] has crossed the [North Pole] reversed-flux area." Our study unfortunately shows that the NMP's drift speed is very sensitive to both the relative position of patches of large secular variation at the core surface with respect to the NMP position, and to the changes in the secular variation at the core surface. Given these conditions, and without a theory describing the evolution of the secular variation at the core surface (which would also have to take into account magnetohydrodynamical processes within the core that are very hard to constrain from surface observations), it seems almost impossible to forecast the future NMP drift speed. It even seems difficult to forecast

the future direction of the NMP drift, although this direction has hardly changed since the end of the 19th century.

## 6. Conclusions

[41] In the present paper we have tried to understand the various mechanisms, both geometrical and physical, that are the cause of the unusually large NMP drift acceleration in the 1990s. The acceleration started in 1989 and ended in 2002, and the total increase in the drift speed was about 45 km/yr. We have reached the following conclusions:

[42] 1. The increase in drift speed of the NMP is related to similar increases in the secular variation of the horizontal magnetic field in the NMP area. This increase was observed in nearby observatories as well as global models. It is particularly large in the component parallel to the direction of the NMP's drift.

[43] 2. The large change in the secular variation of the horizontal components at the Earth's surface in the area of the NMP is caused by a large change in the secular variation of the radial component at the core surface. Within this patch, which is located under the New Siberian Islands, the change over the time interval 1989 to 2002 reaches about 10000 nT/yr. The Green's function relating the field at the core surface and the field at the Earth's surface shows that this effect is maximized by the relative positions of the NMP and the patch under the New Siberian Islands.

[44] 3. The secular variation change at the core surface over 1989–2002 is found to be hemispherically asymmetrical, with the largest values in the Northern hemisphere, and particularly within the patch under the New Siberian Islands and a nearby patch under North Eastern China. A similar asymmetry is found in the secular variation of the  $X$  component at the Earth surface, with maxima in the Canadian Arctic and Eastern Siberia (of about 50 nT/yr).

[45] 4. It is likely that the secular variation under the New Siberian Islands in the 1990s is mostly diffusive and corresponds to the emergence of a new reversed flux patch in this area of the core surface. Such a magnetic flux expulsion could be related to a polar magnetic upwelling within the tangent cylinder, as observed by Aubert *et al.* [2008] in their numerical simulations of the geodynamo. According to this mechanism, the acceleration of the NMP could be a result of a slowdown of the corresponding magnetic upwelling.

[46] 5. The increase in the NMP's drift speed in the 1990s could possibly be related to the 1991 and 1999 (or 2003) geomagnetic jerks, but such a link remains highly speculative in the absence of a theory relating geomagnetic jerks and core processes.

[47] 6. The present state of our knowledge of the core processes that cause the geomagnetic secular variation is not sufficient to allow a reliable prediction of the direction and speed of the NMP.

[48] **Acknowledgments.** The research presented in this paper rely on data collected at magnetic observatories. We thank the national institutes that support them and INTERMAGNET for promoting high standards of magnetic observatory practice ([www.intermagnet.org](http://www.intermagnet.org)). We thank Julien Aubert for useful discussions. We thank two anonymous reviewers for very constructive comments. The research reported here was financially supported by CNES. This is IGP contribution 2624.

## References

- Allan, D. W., and E. C. Bullard (1966), The secular variation of the Earth's magnetic field, *Proc. Cambridge Philos. Soc.*, **62**, 783–809.
- Amit, H., P. Olson, and U. R. Christensen (2007), Tests of core flow imaging methods with numerical dynamos, *Geophys. J. Int.*, **168**, 27–39.
- Aubert, J., J. Aurnou and J. Wicht (2008), The magnetic structure of convection-driven numerical dynamos, *Geophys. J. Int.*, **172**, 945–956.
- Backus, G. E. (1968), Kinematics of geomagnetic secular variation in a perfectly conducting core, *Philos. Trans. R. Soc. London A*, **263**, 239–266.
- Bloxham, J. (1986), The expulsion of magnetic flux from the Earth's core, *Geophys. J. R. Astron. Soc.*, **87**, 669–678.
- Chulliat, A. (2004), Geomagnetic secular variation generated by a tangentially geostrophic flow under the frozen-flux assumption—Part II. Sufficient conditions, *Geophys. J. Int.*, **157**, 537–552.
- Chulliat, A., and G. Hulot (2000), Local computation of the geostrophic pressure at the top of the core, *Phys. Earth Planet. Inter.*, **117**, 309–328.
- Chulliat, A., and N. Olsen (2010), Observation of magnetic diffusion in the Earth's outer core from Magsat, Ørsted and CHAMP data, *J. Geophys. Res.*, **115**, B05105, doi:10.1029/2009JB006994.
- Constable, C. G., R. L. Parker, and P. Stark (1993), Geomagnetic field models incorporating frozen-flux constraints, *Geophys. J. Int.*, **113**, 419–433.
- Courtilot, V., J. Ducruix, and J. -L. Le Mouél (1978), Sur une accélération récente de la variation séculaire du champ magnétique terrestre, *C. R. Acad. Sci. Ser. D*, **287**, 1095–1098.
- Gubbins, D. (2007), Geomagnetic constraints on stratification at the top of the Earth's core, *Earth Planets Space*, **59**, 661–664.
- Gubbins, D., and N. Roberts (1983), Use of the frozen-flux approximation in the interpretation of archaeomagnetic and palaeomagnetic data, *Geophys. J. R. Astron. Soc.*, **73**, 675–687.
- Gubbins, D., and P. H. Roberts (1987), Magnetohydrodynamics of the Earth's core, in *Geomagnetism*, edited by J. A. Jacobs, pp. 1–183, Academic, London.
- Holme, R., and N. Olsen (2006), Core surface flow modelling from high-resolution secular variation, *Geophys. J. Int.*, **166**, 518–528.
- Hulot, G., and A. Chulliat (2003), On the possibility of quantifying diffusion and horizontal Lorentz forces at the Earth's core surface, *Phys. Earth Planet. Inter.*, **135**, 47–54.
- Hulot, G., C. Eymin, B. Langlais, M. Manda, and N. Olsen (2002), Small-scale structure of the geodynamo inferred from Oersted and Magsat satellite data, *Nature*, **416**, 620–623.
- Hulot, G., T. J. Sabaka, and N. Olsen (2007), The present field, in *Geomagnetism, Treatise on Geophysics*, vol. 5, edited by G. Schubert, pp. 33–75, Elsevier, New York.
- Jackson, A., A. R. T. Jonkers, and M. Walker (2000), Four centuries of geomagnetic secular variation from historical records, *Philos. Trans. R. Soc. London A*, **358**, 957–990.
- Jackson, A., C. G. Constable, M. R. Walker, and R. L. Parker (2007), Models of Earth's main magnetic field incorporating flux and radial vorticity constraints, *Geophys. J. Int.*, **171**, 133–144.
- Le Mouél, J.-L. (1984), Outer core geostrophic flow and secular variation of Earth's geomagnetic field, *Nature*, **311**, 734–735.
- Macmillan, S. (1996), A geomagnetic jerk for the early 1990's, *Earth Planet. Sci. Lett.*, **137**, 189–192.
- Manda, M., and E. Dormy (2003), Asymmetric behavior of magnetic dip poles, *Earth Planets Space*, **55**, 153–157.
- Manda, M., E. Bellanger, and J.-L. Le Mouél (2000), A geomagnetic jerk for the end of the 20th century?, *Earth Planet. Sci. Lett.*, **183**, 369–373.
- Newitt, L. R., and C. E. Barton (1996), The position of the north magnetic pole in 1994, *J. Geomag. Geoelectr.*, **48**, 221–232.
- Newitt, L. R., and A. Chulliat (2007), Comment on "Will the magnetic north pole wind up in Siberia?," *Eos Trans. AGU*, **88**, 571.
- Newitt, L. R., M. Manda, L. A. McKee, and J. J. Orgeval (2002), Recent acceleration of the north magnetic pole linked to magnetic jerks, *Eos Trans. AGU*, **83**, 381.
- Newitt, L. R., A. Chulliat, and J. J. Orgeval (2009), Location of the north magnetic pole in April 2007, *Earth Planets Space*, **61**, 703–710.
- Olsen, N., and M. Manda (2007a), Will the magnetic north pole wind up in Siberia?, *Eos Trans. AGU*, **88**, 293.
- Olsen, N., and M. Manda (2007b), Investigation of a secular variation impulse using satellite data: The 2003 geomagnetic jerk, *Earth Planet. Sci. Lett.*, **255**, 94–105.
- Olsen, N., M. Manda, T. J. Sabaka and L. Tøffner-Clausen (2009), CHAOS-2—A geomagnetic field model derived from one decade of continuous satellite data, *Geophys. J. Int.*, **179**, 1477–1487.
- Olson, P., and J. Aurnou (1999), A polar vortex in the Earth's core, *Nature*, **402**, 170–173.

- Pais, A., and G. Hulot (2000), Length of day decade variations, torsional oscillations and inner core superrotation: Evidence from recovered core surface zonal flows, *Phys. Earth Planet. Inter.*, *118*, 291–316.
- Roberts, P. H., and S. Scott (1965), On analysis of the secular variation, *J. Geomag. Geoelectr.*, *17*, 137–151.
- Ross, J. C. (1834), On the position of the north magnetic pole, *Philos. Trans. R. Soc. London*, *124*, 46–51.
- Sabaka, T. J., N. Olsen, and M. Purucker (2004), Extending comprehensive models of the Earth's magnetic field with Ørsted and CHAMP data, *Geophys. J. Int.*, *159*, 521–547.
- Shure, L., R. L. Parker, and G. Backus (1982), Harmonic splines for geomagnetic modelling, *Phys. Earth Planet. Inter.*, *28*, 215–229.
- Wardinski, I., and R. Holme (2006), A time-dependent model of the Earth's magnetic field and its secular variation for the period 1980–2000, *J. Geophys. Res.*, *111*, B12101, doi:10.1029/2006JB004401.
- 
- A. Chulliat and G. Hulot, Equipe de Géomagnétisme, Institut de Physique du Globe de Paris, Université Paris Diderot, INSU, CNRS, 4 Pl. Jussieu, F-75005 Paris, France. (chulliat@ipgp.fr; gh@ipgp.fr)
- L. R. Newitt, Boreal Language and Science Services, 310-1171 Ambleside Dr., Ottawa, ON K2B 8E1, Canada. (boreallanguage@sympatico.ca)